Genome editing of *Pik3cd* impedes abnormal retinal angiogenesis

Wenyi Wu[1,2], Gaoen Ma[3], Hui Qi[4], Lijun Dong[4], Fang Chen[5], [1]Yun Wang, Xingxing Mao[4], Xiaoqing Guo[2], Jing Cui[6], Joanne Aiko Matsubara[6], Bart Vanhaesebroeck[7], Xiaohe Yan[4], Guoming Zhang[4], Shaochong Zhang[4]* and Hetian Lei[4]*

[1]Department of Ophthalmology, Xiangya Hospital, Central South University, Changsha, 410000, China

[2]Schepens Eye Research Institute of Massachusetts Eye and Ear; Department of Ophthalmology, Harvard Medical School, Boston, MA, 02114, United States of America

[3]Department of Ophthalmology, the Third Affiliated Hospital of Xinxiang Medical University, Eye Hospital of Xinxiang Medical University, Xinxiang, 453000, China.

[4]Shenzhen Eye Hospital, Jinan University, Shenzhen Eye Institute, Shenzhen, 518000, China

[5]Huan Key Laboratory of Molecular Precision Medicine, Xiangya Hospital & Hunan Key Laboratory of Medical Genetics, School of Life Sciences, Central South University, Changsha, 410000, China

[6]The University of British Columbia, Vancouver, V5Z 3N9, Canada

[7]Cancer Institute, University College London, London, WC1E 6BT, United Kingdom

*Correspondence: 18 Zetian Road, Shenzhen Eye Hospital, Futian District, Shenzhen, 518000, China.
SZ: zhagngshaochong@gzzoc.com, HL: leithetian18@hotmail.com

Abstract

Abnormal angiogenesis is associated with myriad human diseases including proliferative diabetic retinopathy. Signaling transduction via phosphoinositide 3-kinases (PI3Ks) plays a critical role in angiogenesis. Herein, we showed that p110δ, the catalytic subunit of PI3Kδ, was highly expressed in pathological retinal vascular endothelial cells (ECs) in a mouse model of oxygen-induced retinopathy (OIR) and in fibrovascular membranes from patients with proliferative diabetic retinopathy. To explore novel intervention with PI3Kδ expression, we developed a recombinant dual adeno-associated viral (rAAV) system for delivering CRISPR/Cas9 in which *Streptococcus pyogenes* (Sp) Cas9 expression was driven by an endothelial specific promoter of intercellular adhesion molecule 2 (pICAM2) to edit genomic *Pik3cd*, the gene encoding p110δ. We then demonstrated that infection of cultured mouse vascular endothelial cells with the dual rAAV1s of rAAV1-pICAM2-SpCas9 and rAAV1-SpGuide targeting genomic *Pik3cd* resulted in 80% DNA insertion/deletion in the locus of genomic *Pik3cd* and 70% depletion of p110δ expression. Furthermore, we showed that in the mouse model of OIR editing retinal *Pik3cd* with the dual rAAV1s resulted in not only a significant decrease in p110δ expression, and Akt activation, but also a dramatic reduction in pathological retinal angiogenesis. These findings reveal that *Pik3cd* editing is a novel approach to treating abnormal retinal angiogenesis.

Keywords: AAV-CRISPR/Cas9, genome editing, *Pik3cd*, oxygen-induced retinopathy, retinal angiogenesis

Introduction

Pathological angiogenesis, which is associated with a variety of human diseases including cancer metastasis [1, 2], proliferative diabetic retinopathy (PDR) [3], retinopathy of prematurity (ROP) [4], neovascular age-related macular degeneration (nAMD) [5], pathological myopia choroid neovacularization (PM-CNV) [6] and retinal vein occlusion (RVO) [7], remains a therapeutic challenge. Anti-angiogenic therapy for tumor growth and cancer metastasis is to block the nutrient and oxygen supply to the tumor cells via inhibiting new blood vessels formation [2]. At present, agents targeting vascular endothelial growth factor (VEGF) [8, 9] such as bevascizuman have been approved for cancer treatment, but they are insufficient in many cases to stop cancer progression [10]. In addition, anti-VEGF agents [9, 11] such as aflibercept and ranibizumab, are being used to treat angiogenesis-related eye diseases. However, the repeat intraocular injections are a personal and economic burden along with a risk of infection for the patients [12, 13]. Therefore, novel approaches to blocking pathological angiogenesis are urgently needed.

The approval of gene therapy for *RPE65*-Leber congenital amaurosis (LCA2) [14-17] has highlighted this strategy as a novel approach for the treatment of angiogenesis-associated eye diseases. Ocular diseases are particularly conducive to gene therapy, given the relative accessibility of the eye using established techniques that also allow non-invasive measurement of restoration of visual function to determine therapeutic efficacy. The eye is also immune-privileged, and adeno-associated virus (AAV)-mediated gene therapy of the retina has shown only limited local or systemic immune responses in the form of neutralizing antibodies to the AAV vector or T cell responses to the viral capsid [17, 18]. Use of the recombinant (r)AAV to express soluble Flt-1, the extracellular domain of VEGF receptor (VEGFR)1, has recently entered clinical trials [19, 20] as a single injection approach to achieve long-term efficiency, in this case for the treatment of nAMD.

Targeted gene editing is possibly through induced double-stranded-DNA (dsDNA) breaks in the eukaryotic chromosome. By employing the microbial acquired immune system of CRISPR/Cas, the Cas (e.g. Cas9), a DNA (or RNA) endonuclease under the guidance of a single guide RNA (sgRNA), binds to a DNA sequence complementary to the sgRNA spacer adjacent to a protospacer adjacent motif (PAM). Cas9 senses correct base-pairing, thus activating its RuvC and HNH nuclease domains to cleave target DNA strands, triggering genome editing [18, 21].

Recently genome editing has been employed to deplete crucial genes to treat pathological conditions in a variety of animal models. For instance, VEGF depletion in retinal pigment epithelial (RPE) cells using rAAV-CRISPR/Cas9 has been explored to treat nAMD in a mouse model of laser-induced choroid neovascularization (CNV) [22]. Likewise, VEGFR2 depletion in vascular endothelial cells (ECs) has been harnessed to treat intraocular angiogenesis in mouse models of CNV and oxygen-induced retinopathy (OIR) [23]. These two mouse models have been successfully used in the screening of currently used clinical anti-VEGF agents [24, 25]. However, given that VEGF signaling is also required for neural cell survival [23, 26], an ideal approach would be to inhibit pathological angiogenesis without impacting on normal retinal function.

Phosphoinositide 3-kinases (PI3Ks) phosphorylate the 3′ position of the inositol head group of the phosphatidylinositol (PtdIns) membrane lipids, which serve as ligands and functional regulators of a range of proteins. One major downstream effectors is the Akt serine/threonine kinase that plays a central part in cell survival, growth, metabolism and angiogenesis [27, 28]. PI3Ks include eight isoforms and can be divided into three classes, of which the class I PI3Ks are heterodimers consisting of a p110 catalytic subunit and a regulatory subunit. The class I PI3Ks engage in signaling downstream of tyrosine kinases,

G protein-coupled receptors and monomeric small GTPases. Class I PI3K have four catalytic subunits in mammals, namely p110α, -β, -δ and –γ encoded by the *PIK3CA, -B, -D* and *-G* genes, respectively [29].

We have recently reported that PI3Kδ is highly expressed in vascular ECs in cultured human retinal microvascular endothelial cells (HRECs), and that pharmacological or genetic inactivation of PI3Kδ suppresses pathological retinal angiogenesis in the mouse OIR model[30]. Given the hardly detectable expression of PI3Kδ in mouse photoreceptor cells [30], it is likely that its activity in these cells is not essential. In addition, given that small molecular inhibitors for PI3Kδ (e.g. idelalisib) have a limited half-life in patients, and therefore most likely in vitreous, we thus applied a rAAV-based *Pik3cd* gene editing targeting to long-term dampen p110δ expression to experimentally treat the angiogenesis-related eye diseases, highlighting its potential as a novel approach for inhibiting angiogenesis-associated human diseases including PDR.

Methods

Reagents

Antibodies against p110α, p110β, p110δ, CD31, HIF1α, Akt or phospho-Akt (S473) were from Cell Signaling Technology (Danvers, MA). The primary antibody against β-actin and secondary antibodies of horseradish peroxidase (HRP)-conjugated goat anti-rabbit IgG and anti-mouse IgG were from Santa Cruz Biotechnology (Santa Cruz, CA). Enhanced chemiluminescence substrate for detection of HRP was obtained from Thermo Fisher Scientific (Waltham, MA). Alexa fluorescence-594-conjugated mouse endothelial specific isolectin B4 (IB4) was from Life Technology (Grand Island, NY). High-fidelity Herculase II DNA polymerases were from Agilent Technologies (Santa Clara, CA).

Patient samples

Fibrovascular membranes (FVMs) from patients with PDR were prepared as described previously [30, 31]. An ethical approval was obtained before the initiation of this project from the Vancouver Hospital and University of British Columbia Clinical Research Ethics Board. The University of British Columbia Clinical Research Ethics Board policies comply with the Tri Council Policy and the Good Clinical Practice Guidelines, which have their origins in the ethical principles in the Declaration of Helsinki. Written informed consent was obtained from patients.

DNA constructs

Three 20nt target DNA sequences preceding a 5′-NGG PAM sequence at exon 5 in the C57BL/6J mouse genomic *Pik3cd* locus (NC_000070.6)[32] were selected for generating single-guide RNA (gRNA) for SpCas9 targets using the CRISPR design website (http://crispr.mit.edu). The control sgRNA sequence (5'-TGCGAATACGCCCACGCGAT-3') was designed to target the *lacZ* gene from *Escherichia coli* [33]. The SpGuide vector[34] was modified from the vector (Cat. 60957, addgene) [33] (Cambridge, MA). To construct AAV-SpGuides, the top oligos (ACCG-): 5'- CCCCTGTGGGAGCCCTGTAA -3'(mPK1), 5'-AGAGTGGCTCATACTGTGCA -3' (mPK2), 5'- GCCCTTACAGGGCTCCCACA-3' (mPK3) and bottom oligos: 5'-AAC-20nt-C-3'(20nt: complimentary target *Pik3cd* DNA sequences[35] were annealed and cloned into the pAAV-U6-sgRNA-CMV-GFP vector by *SapI* [23, 30]. DNA synthesis and sequencing were done by Massachusetts General Hospital (MGH) DNA Core Facility (Cambridge, MA).

Cell culture

C57BL/6 mouse primary brain microvascular endothelial cells (MVECs) and human retinal vascular endothelial cells (HRECs) were purchased from Cell Biologics (Chicago, IL) and Cell Systems (Kirkland, WA). These vascular endothelial cells were cultured in the endothelial cell medium with a kit (Cell Applications, San Diego, CA), and their tissue culture dishes were pre-coated with gelatin-based coating solution (Cell Biologics). A human retinal pigment epithelial cell line, ARPE-19, was purchased from America Type Culture Collection (Manassas, VA) and cultured in DMEM/F12 supplemented with 10% fetal bovine serum (FBS); human embryonic kidney (HEK) 293T cells (HEK 293 containing SV40 T-antigen) from ATCC were cultured in high-glucose (4.5 g/l) DMEM supplemented with 10% FBS. All cells were cultured at 37°C in a humidified 5% CO_2 atmosphere [23].

Production of adeno-associated virus

Recombinant AAV2/1 (rAAV1) vectors were produced as described previously[23, 36] in the Gene Transfer Vector Core in Schepens Eye Research Institute of Massachusetts Eye and Ear (Boston, MA). Briefly, triple transfection of AAV package plasmid (AAV2/1), transgene plasmid (pAAV-pICAM2-SpCas9: AAV-SpCas9 [23], pAAV-U6-*Pik3cd*-CMV-GFP: AAV-*Pik3cd* or pAAV-U6-*lacZ*-CMV-GFP: AAV-*lacZ*) and adenovirus helper plasmid were performed in a 10-layer hyper flask containing confluent HEK 293 cells. On day 3 post transfection, the cells and culture medium were harvested and enzymatically treated with Benzonase (EMD Millipore). After high speed centrifugation and filtration, the cell debris was cleared. The viral solution was concentrated by running through tangential flow filtration, and then loaded onto an iodixional gradient column. After one round of ultracentrifugation, the pure vectors were

separated and extracted, then ran through an Amicon Ultra-Centrifugal Filter device (EMD Millipore) for desalting. Both vectors were titrated by TaqMan PCR amplification (Applied Biosystems 7500, Life Technologies), with the primers and probes detecting the transgene. Sodium dodecyl sulfate-polyacrylamide gel electrophoresis (SDS-PAGE) was performed to check the purity of the vectors, which were named rAAV1-SpCas9, rAAV1-*Pik3cd*, and rAAV1-*lacZ* [23].

Western blotting analysis

MVECs at 90% confluency in a 24-well plate were lysed in 1× sample buffer, which was diluted with extraction buffer (10 mM Tris-HCl, pH 7.4, 5 mM EDTA, 50 mM NaCl, 50 mM NaF, 1% Triton X-100, 20 μg/ml aprotinin, 2 mM Na_3VO_4, and 1 mM phenylmethylsulfonyl fluoride) from the 5× protein sample buffer (25 mM EDTA (pH 7.0), 10% SDS), 500 mM dithiothreitol, 50% sucrose, 500 mM Tris-HCl (pH 6.8), and 0.5% bromophenol blue).

Mouse retinas were grounded in the extraction buffer and their lysates were clarified by centrifugation for 10 minutes (min) at 4°C. After quantification with a BCA assay kit (Thermo Fisher Sceientific, Waltham, MA), these clarified lysates were mixed with the 5× protein sample buffer.

The protein samples were boiled for 5 min and then centrifuged for 5 min at 13,000 ×g. Proteins from the centrifuged and heated samples were separated by 10% SDS-PAGE, transferred to polyvinylidene difluoride (PVDF) membranes, and subjected to western blot analyses using the appropriate antibodies. Experiments were repeated at least 3 times. Signal intensity was determined by densitometry using NIH ImageJ software [30].

DNA sequencing

Transduced cells were pelleted for genomic DNA extraction using the QuickExtract DNA Extraction Solution (Epicenter, Chicago, IL) following the manufacturer's protocol. In brief, the pelleted cells were re-suspended in the QuickExtract solution, vortexed for 15 sec, incubated at 65°C for 6 min, vortexed for 15 sec and then incubated at 98°C for 5 min. The genomic region of approximately 300 bp around the PAM was PCR amplified with high-fidelity Herculase II DNA polymerases (Agilent Technologies, Santa Clara, CA). The PCR primers for MVECs and mouse retinas were P33F (forward 5'-GAAGGGCTGGATGTCGCAC-3') and P33R (reverse 5'-CATGGCTAGTCTTCCGGTGT-3'). The PCR products were separated in 2% agarose gel and purified with a gel extraction kit (Thermo Fisher Scientific) for Sanger DNA sequencing and next generation sequencing. DNA sequencing was performed by the MGH DNA core facility [30, 37].

A mouse model of oxygen-induced retinopathy (OIR)

C57BL/6J litters on postnatal day (P) 7 were exposed to 75% O_2 until P12 in an oxygen chamber (Biospherix). Oxygen concentration was monitored daily using an O_2 sensor (Advanced Instruments, GPR-20F) [24]. At P12, the pups were anesthetized by intraperitoneal injection of 50 mg/kg ketamine hydrochloride and 10 mg/kg xylazine. During intravitreal injections, the eyelids of P12 pups were separated by incision. Pupils were dilated using a drop of 1% tropicamide and the eyes were treated with topical proparacaine anesthesia. Intravitreous injections were performed under a microsurgical microscope using glass pipettes with a diameter of approximately 150 μm at the tip after the eye were punctured at the upper nasal limbus using a BD insulin syringe with the BD ultra-fine needle. One μl of both of rAAV1-SpCas9 with rAAV1-*Pik3cd* or rAAV1-*lacZ* (1 μl, 3.0×10^{12} vg/ml) was injected. After the intravitreal injection, the eyes were treated with a triple antibiotic (Neo/Poly/Bac) ointment and kept in room air (21% O_2). At P17, the mice were euthanized and retinas were carefully removed for western blot analysis or fixed in 3.7% paraformaldehyde (PFA). Mice under 6 g of total body weight were excluded from the experiments. Each experiment was at least repeated 3 times in this OIR model. Retinal whole mounts were stained overnight at 4°C with the murine-specific EC marker IB4-Alexa 594 (red) [23]. The images were taken with an EVOS FL Auto microscope.

All the animal experiments followed the guidelines of the Association for Research in Vision and Ophthalmology Statement for the Use of Animals in Ophthalmic and Vision Research. Investigators who conducted analysis were masked as to the treatment groups. All the mice were cared for by following the ACUC protocol approved by the Institutional Animal Care and Use Committee at Schepens Eye Research Institute, and at Jinan University.

RNA sequencing

Retinas carefully isolated from mice intravitreally injected the dual rAAV1 of rAAV1-pICAM2-SpCas9 with with rAAV1-*Pik3cd* or rAAV1-*lacZ* (1 μl, 3.0×10^{12} vg/ml) were sent to Novogene [38, 39] for RNA sequencing analysis, whose report was summarized in the supplemental data. Briefly, RNA-sequencing was performed on the Illumina HiSeq2500 with the sequencing reagents and flow cells that provided up to 300 Gb of sequence information per flow cell. The quality of the total RNA was estimated using the Agilent 2100 Bioanalyzer. For mRNA-seq, 2 rounds of polyA+ selection were performed. We used the stranded mRNA library generation kits per manufacturer's instructions (Agilent, Santa Clara, CA). The cDNA libraries were quantitated using qPCR in a Roche LightCycler 480 with the Kapa Biosystems kit

for library quantitation (Kapa Biosystems, Woburn, MA) before cluster generation. Clusters were produced to yield ~725–825 K clusters per mm^2. Cluster density and quality were determined during the run after the first base addition parameters were assessed. 2 × 50 bp sequencing runs were used to align the cDNA sequences to the reference genome.

Quantification of vaso-obliteration and neovascularization

This was performed as described previously [23]. Briefly, retinal image was imported into Adobe Photoshop CS4, and the Polygonal Lasso tool was used to trace the vascular area of the entire retina. Once the vascular area was highlighted, the number of pixels was obtained. After selecting total retinal area, the lasso tool and the 'subtract from selection' icon to was used to selectively remove the vascularized retina. Leaving behind only the avascular area. Once the avascular region was selected, click the refresh icon again to obtain the number of pixels in the avascular area.

When analyzing NV, the original image was reopened. The magic wand tool was selected from the side tool panel on the left side of the screen. On the top tool panel, the tolerance to a level that will pick up NV was set while excluding normal vessels (beginning at 50). Regions of NV were selected by clicking on them with the magic wand tool. The areas of NV fluoresced more intensely than surrounding normal vessels. When neovessels were selected, the area of interest was zoomed in by holding the 'Alt" key on the keyboard and scrolling up. When all NV was selected and checked, the refresh icon and record the total number of pixels clicked in the NV area[23].

Immunofluorescence

Embedded frozen mouse eyeballs were prepared as described previously [30, 40]. The eyeballs were embedded in O.C.T. on dry ice and sectioned. The slides were fixed in 3.7% formaldehyde/phosphate buffered saline (PBS) for 10 min. Subsequently, the tissues and sections were preincubated with 5% normal goat serum in 0.3% Triton X-100/PBS for 20 min, incubated with IB4 (1:100 dilution) for 1 hour (h). Following 3 washes with PBS, the slides were mounted with a mount medium containing 4',6-diamidino-2-phenylindole (DAPI) (Vector Laboratories Inc. Burlingame, CA) and photographed using an EVOS FL Auto microscope [30].

FVMs and eyeball sections on slides were fixed in 3.7% formaldehyde/PBS for 10 min. Subsequently, the sections and FVMs were preincubated with 5% normal goat serum in 0.3% Triton X-100/PBS for 30 min, incubated with primary antibodies against p110δ (1:200, rabbit) and CD31 (1:200, mouse) or a normal rabbit (or mouse) IgG overnight at 4°C. After 3 washes with 0.3% Triton X-100/PBS,

the tissues and sections were incubated with fluorescently-labeled secondary antibodies Dylight 549 (Vector laboratories, Inc. Burlingame, CA) and Dylight 480 (1:300 dilution in blocking buffer) for 30 min. Following 3 washes with 0.3% Triton X-100/PBS, the slides were mounted with a mount medium containing 4',6-diamidino-2-phenylindole (DAPI) and photographed under a fluorescence microscope [23, 40, 41].

Data preparation and associations of *PIK3CD* with *Hif-1A*

The transcriptome profiles and corresponding clinical information on PDR patients were downloaded from the Genomic Data of GEO (https://www.ncbi.nlm.nih.gov/geo/) on Jun 16, 2021. The transcriptome data involved 80 samples from two distinct retinal sample sites (macula, periphery) in diabetes with retinopathy or not and 20 normal tissues[42]. The "coR" R package install with ggplot2 was used to assess Spearman correlation values between *PIK3CD* and *Hif-1A* using the transcriptome data.

Statistics

The data from 3 independent experiments were analyzed using an unpaired t-test between two groups, and one-way ANOVA among more than two groups. For animal experiments the data from at least 6 mice were used for the statistical analysis. All data were analyzed using a masked procedure. P values < 0.05 were considered statistically significant.

Results

Hypoxia heightens p110δ expression in the mouse retinas

p110δ is expressed at low levels in cells other than leukocytes such as ECs, but its expression can be induced in ECs by tumor necrosis factor (TNF)α [43, 44]. Our previous findings have demonstrated that high glucose induces p110δ expression in cultured human retinal microvascular ECs （HRECs） [30]. Based on the notion that diabetic hyperglycemia can cause retinal ischemia, leading to hypoxia [45], we hypothesized that hypoxia might also be able to enhance p110δ expression in the retina. Indeed, western blot analysis of retinal lysates from P17 mice with or without experiencing OIR showed that hypoxia significantly promoted p110δ expression in the mouse retina without altering expression of p110α and p110β (Fig. 1A, B). In addition, p110δ was expressed at low levels in mouse retinal cone cells and high levels in mouse macrophages (Fig. 1A, B), in agreement with our previous findings[30]. To reveal if p110δ

was expressed in pathological ECs *in vivo*, we examined p110δ expression in mouse retinas of the OIR model at P17, a time when pathological angiogenesis reaches a peak in this model[24]. High p110δ expression was confirmed by immunofluorescence in pathological ECs (Fig. 2A-F); notably, its expression was hardly detectable in normal mouse retinal ECs (Supplemental figure 1). Furthermore, p110δ was also highly expressed in ECs of fibrovascular membranes from patients with PDR (Fig. 2G-L), consistent with our previous findings[30]. Notably, pharmacological and genetic inactivation of PI3Kδ suppresses retinal pathological angiogenesis [30], suggesting *Pik3cd* editing to impede p110δ expression as a novel approach for hindering pathological angiogenesis.

In vitro genomic *Pik3cd* editing

We previously established a dual rAAV system for *Streptococcus pyogenes* (Sp) Cas9 expression specifically in ECs. In this system, expression of SpCas9 is driven by the endothelial-specific promoter of the intercellular adhesion molecule 2 (ICAM 2), namely pAAV-pICAM2-SpCas9, and in the SpGuide there is expression of green fluorescence protein (GFP) driven by a cytomegalovirus (CMV) promoter [23]. In order to edit mouse *Pik3cd*, we selected three gRNAs from mouse genomic loci and cloned them into the AAV-SpGuide vector by *SapI,* respectively, as shown previously[23, 33].

We first analyzed the editing efficiency of the dual AAVs in cultured ECs. Primary C57BL/6 mouse brain microvascular ECs (MVECs) were electroporated with plasmids of rAAV-pICAM2-SpCas9 in combination with plasmids of rAAV-mPK1, -mPK2, -mPK3 or -*lacZ* as a control. The mPK2–sgRNA to target mouse *Pik3cd* was found able to guide SpCas9 to cleave the genomic *Pik3cd* locus in MVECs, resulting in DNA mutations around the protospacer adjacent motif (PAM) (Fig. 3A, B) and depletion of p110δ in about 70% of the cells transduced with mPK2-sgRNA compared with those with the control *lacZ*-sgRNA (Fig. 3C, D). For *in vivo* studies, we next used the plasmids of rAAV-mPK2-sgRNA, rAAV-*lacZ*-sgRNA and rAAV-pICAM2-SpCas9 to produce their rAAV1 viruses, respectively, given that rAAV1 transduces ECs with high efficiency[23].

Editing *Pik3cd* suppresses abnormal retinal angiogenesis in a mouse model of OIR

Before testing the editing efficiency of the dual recombinant (r)AAV1s *in vivo*, we examined if the promoter of pICAM2 was specific for vascular endothelial cells in vitro. As shown in Fig. 4A-B, GFP expression driven by pICAM2 was hardly detectable in ARPE-19 cells, but it was detected in HRECs; in addition, GFP expression driven by the CMV promoter was very strong in ARPE-19 cells (Fig. 4C), demonstrating pICAM2 was specific for vascular endothelial cells. We next evaluated whether rAAV1

could transduce ECs by intravitreal injection of rAAV1-CMV-GFP into mouse eyes at P12 experiencing the OIR model, followed by IB4 staining of frozen eye sections at P17 (Fig. 4D-G). These analyses showed that rAAV1 was able to transduce vascular ECs of neovascularization induced by hypoxia in the OIR, in agreement with our previous findings [23].

Subsequently, we intravitreally injected rAAV1-pICAM2-SpCas9 together with equal amount of rAAV1-*Pik3cd*-sgRNA or *lacZ*-sgRNA (1 μl, 3.0 x 10^{12} vg/ml) into P12 mice in the OIR model, followed by analysis of the retinas at P17. IB4 staining of whole-mount retinas revealed a significant decrease in the number of preretinal tufts (reflective of pathological neovascularization) [24] (Fig. 5A, B, and sFig. 3) in the retinas from mice injected with *Pik3cd*-sgRNA compared with those injected with control *lacZ*-sgRNA, but the avascular areas between these groups were not significantly changed (Fig. 5A, C). Gene editing efficiency tested by next generation sequencing (NGS) of retinas showed a 2.05% insertion and 0.68% deletion with *Pik3cd*-sgRNA (Fig. 5D). Western blot analysis indicated there was 30 ±0.5% reduction in p110δ expression in the retinas from mice injected with rAAV1-*Pik3cd*-sgRNA compared with those with rAAV1-*lacZ*-sgRNA with no significant changes in p110α and p110β expression (Fig. 5E, F). Taken together, these data in Figure 5 demonstrate that *Pik3cd* editing in vascular ECs reduced p110δ expression and suppressed hypoxia-induced pathological neovascularization in the mouse model of OIR.

Next, RNA sequencing was used to examine which signaling pathways were impacted after genomic editing of endothelial p110δ in the retinas from P17 mice experiencing OIR. As shown in Fig. 6A and sFig. 4-9, *Pik3cd* editing affected 20 signaling pathways, of which PI3K/Akt signaling was downregulated as expected, but we also found that HIF1 signaling was the strongest downregulated candidate among these signaling pathways (Fig. 6A). Western blot analysis confirmed that there was a significant decrease in Akt activation and HIF-1α expression after *Pik3cd* editing in retinal vascular ECs in the OIR mice (Fig. 6B), suggesting that *Pik3cd* editing resulted in suppression of pathological retinal angiogenesis by reducing HIF1α expression via blocking hypoxia-induced Akt activation.

Discussion

Here we report that *Pik3cd* editing with a dual rAAV1 system to deliver SpCas9 and its gRNA into mouse ECs suppresses p110δ expression and attenuates pathological angiogenesis in the mouse model of

OIR. These data are in line with a previous study demonstrating that inactivation of PI3Kδ using pharmacological or genetic approaches inhibits pathological angiogenesis in the OIR model [30]. Importantly, in this study we uncovered that hypoxia enhances p110δ expression in vascular ECs (Figs. 1 - 2), and the purpose of this research was to deplete expression of p110δ in these ECs to prevent abnormal neovascularization.

In Figure 5, there are only about 2.7% of insertions and deletions around the PAM, which still led to significant suppression of hypoxia-induced retinal pathological angiogenesis, consistent with our similar findings for VEGFR2 [23]. This could be explained by the possibility that rAAV1 preferentially infects pathological ECs, which constitute only a small fraction of whole retinal genomic DNA; however, the specific receptor (s) that rAAV1[46] prefer to engage for rAAV1 to enter pathological ECs remain elusive and this question is worth further investigation. This treatment was also found to give rise to biological effects already only 5 days after rAAV1 injection. This could be explained by our observations (Supplemental Fig. 2) that it is possible to detect AAV1 infection in cultured ECs within 6 hours *in vitro* and vascular ECs within 24 hours *in vivo*. Upon intravitreal injection of AAV1 at P12, i.e. when the mice just came out of the oxygen chamber, the abnormal ECs had not grown yet, but when these began to expand the next day, the rAAV1s were already present for infection, allowing to induce a decrease in expression of p110δ to suppress hypoxia-induced Akt activation and pathological ECs expansion.

Given the instability of HIF1α, which is regulated primarily by stabilization of the expressed protein, the Western blot indicates HIF1α protein level (Fig. 6) may not be a direct indicator of HIF1α expression. Intriguingly, analysis of the transcriptome data, which were downloaded from the Genomic Data of GEO (https://www.ncbi.nlm.nih.gov/geo/) and involved 80 samples from two distinct retinal sample sites (macula, periphery) in diabetes with retinopathy or not and 20 normal tissues[42], shows significantly positive correlation between *PIK3CD* and *Hif-1A* expression (Fig. 7A). These data are consistent with our findings that in the mouse model of OIR *Pik3cd* editing attenuates HIF1α expression in the retina (Fig. 6) and that inactivation of PI3Kδ decreases VEGF production in the vitreous [30]. Thereby, we propose that in the retina hypoxia-induced expression of HIF1α is modulated by the signaling pathway of PI3Kδ and Akt (Fig. 7B), and that Akt regulates of HIF1α expression via activating NFκB based on previous investigations [28,29,47].

PI3Ks are major intracellular lipid enzymes, which transduce extracellular signals to the inside of cells [29]. Akt is a major effector of PI3Ks and plays a central role in angiogenesis [27]. Our previous findings demonstrated that PI3Kδ in vascular ECs mediates Akt activation downstream of multiple angiogenesis-

enhancing factors including VEGF, bFGF and EGF. Hypoxia can induce production of these proangiogenic factors [30]. In line with these data, *Pik3cd* editing can suppress activation of Akt induced by multiple growth factors in response to hypoxia. In addition, PI3Kδ expression is extremely low in mouse photoreceptors compared to ECs [30]. In this way, anti-PI3Kδ is superior to anti-VEGF to only inhibit pathological angiogenesis. Taken together, editing *Pik3cd* is a novel approach with high potential to treat pathological angiogenesis, such as PDR, ROP and nAMD.

A major disadvantage of this genome editing strategy is the generation of genomic alterations such as insertions and deletions. Generation of a kinase-inactive mutant of $p110\delta^{D910A}$ by prime editing[48] might therefore be a better approach. In addition, kinase-dead Cas9[49] could also be used to target and functionally disable the *Pik3cd* promoter. These potential strategies are currently being actively explored in our laboratory.

AAV-based gene therapy is expected to be most advantageous in the treatment of inherited retinal diseases including inherited retinal degenerative disease [17, 18, 20]. In this study, we used this AAV approach to treat acquired angiogenesis-related ocular disease, aiming to decrease the frequency of intravitreally administration of anti-VEGF agents and to treat those patients who suffer from these eye diseases but do not respond to the anti-VEGF therapy. Our dual AAVs with an EC-specific promoter pICAM2 to drive SpCas9 expression is not expected to affect other cells, resulting in less potential side effects in the eye. However, off-target effects associated with prolonged Cas9 expression will need to be monitored. Overall, our results provide evidence for *Pik3cd* editing as a novel approach to prevent abnormal retinal angiogenesis.

Data and Resource Availability

The datasets generated during and/or analyzed during the current study are available from the corresponding author upon reasonable request. The [RESOURCE] generated during and/or analyzed during the current study is available from the corresponding author upon reasonable request.

Conflict of interests

HL has a patient application of the dual AAV vectors related to this article, and BV is a consultant for iOnctura (Geneva, Switzerland), Venthera (Palo Alto. US), Olema Pharmaceutical (San Francisco, US) as well as has received speaker fees from Gilead (Foster City, US). All other authors declare no conflict of interests.

Funding

This work was supported by National Natural Science Foundation of China (82070989) to HL, Sanming Project of Medicine in Shenzhen (SZSM202011015) to YX, GZ, SZ and HL, China Scholarship Council to WW, Central South University student innovation project 2016zzts148 to WW, National Natural Science Foundation of China (81900893, 8227109) to WW, and the Science and Technology Plan Project of Hunan Province (2019RS2011) to WW. No funding bodies had any role in study design, data collection and analysis, decision to publish, or preparation of the manuscript.

Acknowledgements: Dr. Hetian Lei is the guarantor of this work, and has full access to all the data in the study and takes responsibility for the integrity of the data and the accuracy of the data analysis. Authors thank Dr. Joanne A Matsubara of the University of British Columbia, Canada for providing samples of fibrovascular membranes from patients with proliferative diabetic retinopathy.

Author contributions: WW, GM, HQ, LD, FC, YW, XG and XM performed the experiments and analyzed the results; JC and JM provided patient samples; BV, XY, and GZ revised the manuscript; SZ and HL conceived the experiments, analyzed the data and wrote the manuscript.

References

[1] Folkman J: Tumor angiogensis:therapeutic implications. N Engl J Med 1971, 285:1182-6.
[2] Folkman J: Angiogenesis in cancer, vascular, rheumatoid and other disease. Nat Med 1995, 1:27-31.
[3] Cabrera AP, Monickaraj F, Rangasamy S, Hobbs S, McGuire P, Das A: Do Genomic Factors Play a Role in Diabetic Retinopathy? Journal of clinical medicine 2020, 9.
[4] Hansen ED HM: A review of treatment for retinopathy of prematurity. Expert Rev Ophthalmol 2019, 14:73-87.
[5] Miller JW: Developing Therapies for Age-related Macular Degeneration: The Art and Science of Problem-solving: The 2018 Charles L. Schepens, MD, Lecture. Ophthalmol Retina 2019, 3:900-9.
[6] Mimura R, Mori K, Torii H, Nagai N, Suzuki M, Minami S, Ozawa Y, Kurihara T, Tsubota K: Ultra-Widefield Retinal Imaging for Analyzing the Association Between Types of Pathological Myopia and Posterior Staphyloma. Journal of clinical medicine 2019, 8.
[7] Zhu DD, Liu X: Neutrophil/Lymphocyte Ratio and Platelet/Lymphocyte Ratio in Branch Retinal Vein Occlusion. J Ophthalmol 2019, 2019:6043612.

[8] Senger DR, Galli SJ, Dvorak AM, Perruzzi CA, Harvey VS, Dvorak HF: Tumor cells secrete a vascular permeability factor that promotes accumulation of ascites fluid. Science 1983, 219:983-5.
[9] Ferrara N, Henzel WJ: Pituitary follicular cells secrete a novel heparin-binding growth factor specific for vascular endothelial cells. Biochemical and biophysical research communications 1989, 161:851-8.
[10] Lopes-Coelho F, Martins F, Pereira SA, Serpa J: Anti-Angiogenic Therapy: Current Challenges and Future Perspectives. Int J Mol Sci 2021, 22.
[11] Ferrara N HK, Gerber HP, Novotny W.: Discovery and development of bevasizumab, an anti-VEGF antibody for treating cancer. Nature reviews Drug discovery 2004, 3:391-400.
[12] Bhisitkul RB, Desai SJ, Boyer DS, Sadda SR, Zhang K: Fellow Eye Comparisons for 7-Year Outcomes in Ranibizumab-Treated AMD Subjects from ANCHOR, MARINA, and HORIZON (SEVEN-UP Study). Ophthalmology 2016, 123:1269-77.
[13] Grunwald JE, Pistilli M, Daniel E, Ying GS, Pan W, Jaffe GJ, Toth CA, Hagstrom SA, Maguire MG, Martin DF, Comparison of Age-Related Macular Degeneration Treatments Trials Research G: Incidence and Growth of Geographic Atrophy during 5 Years of Comparison of Age-Related Macular Degeneration Treatments Trials. Ophthalmology 2017, 124:97-104.
[14] Hauswirth WW, Aleman TS, Kaushal S, Cideciyan AV, Schwartz SB, Wang L, Conlon TJ, Boye SL, Flotte TR, Byrne BJ, Jacobson SG: Treatment of leber congenital amaurosis due to RPE65 mutations by ocular subretinal injection of adeno-associated virus gene vector: short-term results of a phase I trial. Human gene therapy 2008, 19:979-90.
[15] Ruan GX, Barry E, Yu D, Lukason M, Cheng SH, Scaria A: CRISPR/Cas9-Mediated Genome Editing as a Therapeutic Approach for Leber Congenital Amaurosis 10. Mol Ther 2017, 25:331-41.
[16] Maeder ML, Stefanidakis M, Wilson CJ, Baral R, Barrera LA, Bounoutas GS, Bumcrot D, Chao H, Ciulla DM, DaSilva JA, Dass A, Dhanapal V, Fennell TJ, Friedland AE, Giannoukos G, Gloskowski SW, Glucksmann A, Gotta GM, Jayaram H, Haskett SJ, Hopkins B, Horng JE, Joshi S, Marco E, Mepani R, Reyon D, Ta T, Tabbaa DG, Samuelsson SJ, Shen S, Skor MN, Stetkiewicz P, Wang T, Yudkoff C, Myer VE, Albright CF, Jiang H: Development of a gene-editing approach to restore vision loss in Leber congenital amaurosis type 10. Nat Med 2019, 25:229-33.
[17] Garafalo AV, Cideciyan AV, Heon E, Sheplock R, Pearson A, WeiYang Yu C, Sumaroka A, Aguirre GD, Jacobson SG: Progress in treating inherited retinal diseases: Early subretinal gene therapy clinical trials and candidates for future initiatives. Prog Retin Eye Res 2019:100827.
[18] Wang D, Zhang F, Gao G: CRISPR-Based Therapeutic Genome Editing: Strategies and In Vivo Delivery by AAV Vectors. Cell 2020, 181:136-50.

[19] Constable IJ, Pierce CM, Lai CM, Magno AL, Degli-Esposti MA, French MA, McAllister IL, Butler S, Barone SB, Schwartz SD, Blumenkranz MS, Rakoczy EP: Phase 2a Randomized Clinical Trial: Safety and Post Hoc Analysis of Subretinal rAAV.sFLT-1 for Wet Age-related Macular Degeneration. EBioMedicine 2016, 14:168-75.
[20] Bulcha JT, Wang Y, Ma H, Tai PWL, Gao G: Viral vector platforms within the gene therapy landscape. Signal Transduct Target Ther 2021, 6:53.
[21] Knott GJ, Doudna JA: CRISPR-Cas guides the future of genetic engineering. Science 2018, 361:866-9.
[22] Kim E, Koo T, Park SW, Kim D, Kim K, Cho HY, Song DW, Lee KJ, Jung MH, Kim S, Kim JH, Kim JH, Kim JS: In vivo genome editing with a small Cas9 orthologue derived from Campylobacter jejuni. Nature communications 2017, 8:14500.
[23] Huang X, Zhou G, Wu W, Duan Y, Ma G, Song J, Xiao R, Vandenberghe L, Zhang F, D'Amore PA, Lei H: Genome editing abrogates angiogenesis in vivo. Nature communications 2017, 8:112.
[24] Connor KM, Krah NM, Dennison RJ, Aderman CM, Chen J, Guerin KI, Sapieha P, Stahl A, Willett KL, Smith LE: Quantification of oxygen-induced retinopathy in the mouse: a model of vessel loss, vessel regrowth and pathological angiogenesis. Nat Protoc 2009, 4:1565-73.
[25] Lambert V, Lecomte J, Hansen S, Blacher S, Gonzalez ML, Struman I, Sounni NE, Rozet E, de Tullio P, Foidart JM, Rakic JM, Noel A: Laser-induced choroidal neovascularization model to study age-related macular degeneration in mice. Nat Protoc 2013, 8:2197-211.
[26] Shen J, Xiao R, Bair J, Wang F, Vandenberghe LH, Dartt D, Baranov P, Ng YSE: Novel engineered, membrane-localized variants of vascular endothelial growth factor (VEGF) protect retinal ganglion cells: a proof-of-concept study. Cell Death Dis 2018, 9:1018.
[27] Dimmeler S, Zeiher AM: Akt takes center stage in angiogenesis signaling. Circ Res 2000, 86:4-5.
[28] Toker A, Dibble CC: PI 3-Kinase Signaling: AKTing up inside the Cell. Mol Cell 2018, 71:875-6.
[29] Bilanges B, Posor Y, Vanhaesebroeck B: PI3K isoforms in cell signalling and vesicle trafficking. Nature reviews Molecular cell biology 2019, 20:515-34.
[30] Wu W, Zhou G, Han H, Huang X, Jiang H, Mukai S, Kazlauskas A, Cui J, Matsubara JA, Vanhaesebroeck B, Xia X, Wang J, Lei H: PI3Kdelta as a Novel Therapeutic Target in Pathological Angiogenesis. Diabetes 2020, 69:736-48.
[31] Cui J, Lei H, Samad A, Basavanthappa S, Maberley D, Matsubara J, Kazlauskas A: PDGF receptors are activated in human epiretinal membranes. Exp Eye Res 2009, 88:438-44.

[32] Huang X, Zhou G, Wu W, Ma G, D'Amore PA, Mukai S, Lei H: Editing VEGFR2 Blocks VEGF-Induced Activation of Akt and Tube Formation. Invest Ophthalmol Vis Sci 2017, 58:1228-36.
[33] Swiech L, Heidenreich M, Banerjee A, Habib N, Li Y, Trombetta J, Sur M, Zhang F: In vivo interrogation of gene function in the mammalian brain using CRISPR-Cas9. Nature biotechnology 2015, 33:102-6.
[34] Sanjana NE, Shalem O, Zhang F: Improved vectors and genome-wide libraries for CRISPR screening. Nat Methods 2014, 11:783-4.
[35] Okkenhaug K, Bilancio A, Farjot G, Priddle H, Sancho S, Peskett E, Pearce W, Meek SE, Salpekar A, Waterfield MD, Smith AJ, Vanhaesebroeck B: Impaired B and T cell antigen receptor signaling in p110delta PI 3-kinase mutant mice. Science 2002, 297:1031-4.
[36] Tabebordbar M, Zhu K, Cheng JK, Chew WL, Widrick JJ, Yan WX, Maesner C, Wu EY, Xiao R, Ran FA, Cong L, Zhang F, Vandenberghe LH, Church GM, Wagers AJ: In vivo gene editing in dystrophic mouse muscle and muscle stem cells. Science 2016, 351:407-11.
[37] Han H, Chen N, Huang X, Liu B, Tian J, Lei H: Phosphoinositide 3-kinase delta inactivation prevents vitreous-induced activation of AKT/MDM2/p53 and migration of retinal pigment epithelial cells. J Biol Chem 2019, 294:15408-17.
[38] Wang Z, Gerstein M, Snyder M: RNA-Seq: a revolutionary tool for transcriptomics. Nat Rev Genet 2009, 10:57-63.
[39] Love MI, Huber W, Anders S: Moderated estimation of fold change and dispersion for RNA-seq data with DESeq2. Genome Biol 2014, 15:550.
[40] Lei H, Romeo G, Kazlauskas A: Heat shock protein 90alpha-dependent translocation of annexin II to the surface of endothelial cells modulates plasmin activity in the diabetic rat aorta. Circ Res 2004, 94:902-9.
[41] Lei H, Rheaume MA, Cui J, Mukai S, Maberley D, Samad A, Matsubara J, Kazlauskas A: A novel function of p53: a gatekeeper of retinal detachment. Am J Pathol 2012, 181:866-74.
[42] Becker K, Klein H, Simon E, Viollet C, Haslinger C, Leparc G, Schultheis C, Chong V, Kuehn MH, Fernandez-Albert F, Bakker RA: In-depth transcriptomic analysis of human retina reveals molecular mechanisms underlying diabetic retinopathy. Sci Rep 2021, 11:10494.
[43] Vanhaesebroeck B, Welham MJ, Kotani K, Stein R, Warne PH, Zvelebil MJ, Higashi K, Volinia S, Downward J, Waterfield MD: P110delta, a novel phosphoinositide 3-kinase in leukocytes. Proc Natl Acad Sci U S A 1997, 94:4330-5.

[44] Whitehead MA, Bombardieri M, Pitzalis C, Vanhaesebroeck B: Isoform-selective induction of human p110delta PI3K expression by TNFalpha: identification of a new and inducible PIK3CD promoter. Biochem J 2012, 443:857-67.
[45] Geraldes P, Hiraoka-Yamamoto J, Matsumoto M, Clermont A, Leitges M, Marette A, Aiello LP, Kern TS, King GL: Activation of PKC-delta and SHP-1 by hyperglycemia causes vascular cell apoptosis and diabetic retinopathy. Nat Med 2009, 15:1298-306.
[46] Cronin T, Vandenberghe LH, Hantz P, Juttner J, Reimann A, Kacso AE, Huckfeldt RM, Busskamp V, Kohler H, Lagali PS, Roska B, Bennett J: Efficient transduction and optogenetic stimulation of retinal bipolar cells by a synthetic adeno-associated virus capsid and promoter. EMBO Mol Med 2014, 6:1175-90.
[47] Kinose Y, Sawada K, Makino H, Ogura T, Mizuno T, Suzuki N, Fujikawa T, Morii E, Nakamura K, Sawada I, Toda A, Hashimoto K, Isobe A, Mabuchi S, Ohta T, Itai A, Morishige K, Kurachi H, Kimura T: IKKbeta Regulates VEGF Expression and Is a Potential Therapeutic Target for Ovarian Cancer as an Antiangiogenic Treatment. Mol Cancer Ther 2015, 14:909-19.
[48] Anzalone AV RP, Davis JR, Sousa AA, Koblan LW, Levy JM, Chen PJ, Wilson C, Newby GA, Raguram A, Liu DR.: Search-and-replace genome editing without double-strand breaks or donor DNA. Nature 2019, 576:149-57.
[49] Gjaltema RAF, Schulz EG: CRISPR/dCas9 Switch Systems for Temporal Transcriptional Control. Methods Mol Biol 2018, 1767:167-85.

Figure legends

Figure 1. Hypoxia enhances p110δ expression in mouse retinas

A. Lysates of a mouse macrophage cell line RAW264.7 (RAW), an immortalized cone photoreceptor cell line (661W cells) and retinas from the 17 day- old C57BL/6J mice with or without experiencing OIR were subjected to western blot analysis using indicated antibodies.

B. The intensity of the p110δ bands in (A) was firstly normalized to that of the corresponding β-actin bands. Each bar graph indicates mean ± SD of 3 independent experiments (fold). ** and *** indicate significant difference ($p < 0.01$ and 0.001) between two compared groups using one-way ANOVA followed by a Tukey post test. RA: room air, OIR: oxygen-induced retinopathy.

Figure 2. Expression of p110δ in pathological retinal ECs

A-F. P17 eyeballs from the euthanized C57BL/6J mice experiencing OIR were fixed and the whole retinas were stained with an antibody against p110δ and a mouse EC marker IB4, or normal IgG and IB4. Red and green signals indicate expression of p110δ and IB4, respectively. Shown is a representative of 6 mice. Single arrowhead: pathological ECs, double arrowheads: normal ECs. Scale bar: 50 μm.

G-L. Fibrovascular membranes (FVMs) from PDR patients on slides were subjected to immunofluorescence analysis using antibodies against control antibodies (rabbit and mouse) IgG (E-G) or against p110δ and CD31 (H-J). Red and green signals indicate expression of p110δ and CD31, respectively, in comparison to the non-immune IgG stained control. Blue signals are from nucleus staining with DAPI. This is a representative of 3 independent experiments using different sample sources (FVMs from 3 PDR patients). Blue arrows point to enlarged photos, and white arrows point to representative ECs. The images were taken under immunofluorescence microscope. Scale bar: 50 μm.

Figure 3. AAV-CRISPR/Cas9-mediated depletion of p110δ *in vitro*

A. Graphical representation of a mouse *Pik3cd*-targeted locus at exon 5. The oligos of mPK2 (under the green line) and its compliment were annealed and cloned into the SpGuide vector by *SapI*. The PAM is marked in blue. PAM: protospacer adjacent motif.

B. Schematic of AAV-SpGuide and AAV-SpCas9. ITR: inverted terminal repeat; U6: a promoter of polymerase III; CMV: a promoter of cytomegalovirus; GFP: green fluorescent protein. pICAM2: an endothelial-specific promoter of intercellular adhesion molecule 2.

C. Sanger DNA sequencing was conducted on PCR products amplified from the genomic *Pik3cd* loci of MVECs, which were transduced by rAAV1 -SpCas9 plus rAAV1-*lacZ*-sgRNA (*lacZ*) or rAAV1-mPK2-sgRNA (mPK2).

D. Depletion of p110δ expression in MVECs using AAV-CRISPR/Cas9. Total cell lysates from the transduced MVECs with rAAV1-pICAM2-SpCas9 together with rAAV1-sgRNA-*lacZ* or *Pik3cd* were subjected to western blot analysis with antibodies against p110δ and β-actin. The bar graphs are mean ± standard deviation (SD) of three independent experiments. "***" indicates a significant difference betwn the compared two groups using an unpaired t test. $p < 0.001$.

Figure 4. Transduction of ECs with rAAV1 in vitro and in vivo

A-B. ARPE-19 cells (a cell line of retinal pigment epithelial cells) (A) and human retinal micovascular endothelial cells (HRECs) (B) were infected with rAAV1-pICAM2-GFP and photographed in an immunofluorescence microscope after infection for 48 hours. Scale bar: 200 μm.

C. ARPE-19 cells were infected with rAAV1-CMV-GFP and photographed in an immunofluorescence microscope after infection for 48 hours. Scale bar: 100 μm.

D-G. Eyeball sections from P17 OIR mice, which were intravitreally injected with rAAV1-CMV-GFP (1 μl, 3.0×10^{12} vg/ml) at P12, were stained with IB4 (red) and photographed under an immunofluorescence microscope. Images were taken under TxRed channel (D) & GFP channel (E). F: Merged image of D and E. G: Merged image of D, E and DAPI. Scale bar: 200 μm. Arrows point to the merger of ECs (red) and AAV-infected cells (GFP). Scale bar: 200 μm

Figure 5. Editing genomic *Pik3cd* attenuates hypoxia-induced angiogenesis

A. Litters of P12 mice that had been exposed to 75% O_2 for 5 days were injected intravitreally with 1 μl (3.0×10^{12} vg/ml) containing equal rAAV1-SpCas9 and rAAV1-*lacZ* (*lacZ*) or rAAV1-mPK2 (mPK2). On P17, whole-mount-retinas were stained with IB4. lacZ and mPK2 indicate retinas from the rAAV1-SpCas9/lacZ and mPK2-injected mice, respectively.

B. Analysis of avascular areas from the IB4 stained retinas (n=6). "**" indicates significant difference using an unpaired t test. $p < 0.01$.

C. Analysis of NV areas from the IB4 stained retinas (n=6). ns: not significant.

D. NGS analysis of indels. The DNA fragments around the PAM sequences were PCR amplified from genomic DNA of the rAAV1- SpCas9/-*lacZ* or –mPK2-injected retinas, and then subjected to NGS.

E. The lysates of the rAAV1-SpCas9/lacZ or –mPK2-injected retinas were subjected to western blot analysis using the indicated antibodies. The bar graph data below HIF1α blots are mean ± SD of 3 retinas. "***" indicates significant difference using an unpaired t test. p< 0.001.

F. The bar graph data are mean ± SD of 3 retinas. "***" indicates significant difference using an unpaired t test. p< 0.001. ns: not significant.

Figure 6. Editing genomic *Pik3cd lessens hypoxia-induced Akt activation and HIF1α expression*

A. RNA sequencing analysis of signaling pathways affected by genomic *Pic3cd.*

B. The lysates of the rAAV1-SpCas9/-*lacZ* or –mPK2-injected retinas were subjected to western blot analysis using the indicated antibodies. The bar graph data from Akt and HIF1α blots are mean ± SD of 3 retinas. "***" indicates significant difference using an unpaired t test. p< 0.001.

Figure 7. Diagram of a potential mechanism of PI3Kδ in pathological angiogenesis

A. Positive correlation of *PIK3*CD with *Hif-1A* in retinas from patients with PDR. The transcriptome profiles and corresponding clinical information on PDR patients were downloaded from the Genomic Data of GEO (https://www.ncbi.nlm.nih.gov/geo/). The "coR" R package install with ggplot2 was used to assess Spearman correlation values between *PIK3CD* and *Hif-1A* using the transcriptome data.

B. Schematic illustration of a potential mechanism of PI3Kδ in pathological angiogenesis. Hypoxia induces activation of the signaling pathway of PI3Kδ and Akt, enhancing expression of HIF1α and VEGF probably via NF κ B, resulting in pathological angiogenesis, and inhibition of PI3Kδ leads to attenuation of the abnormal angiogenesis.

Figures

Figure 1.

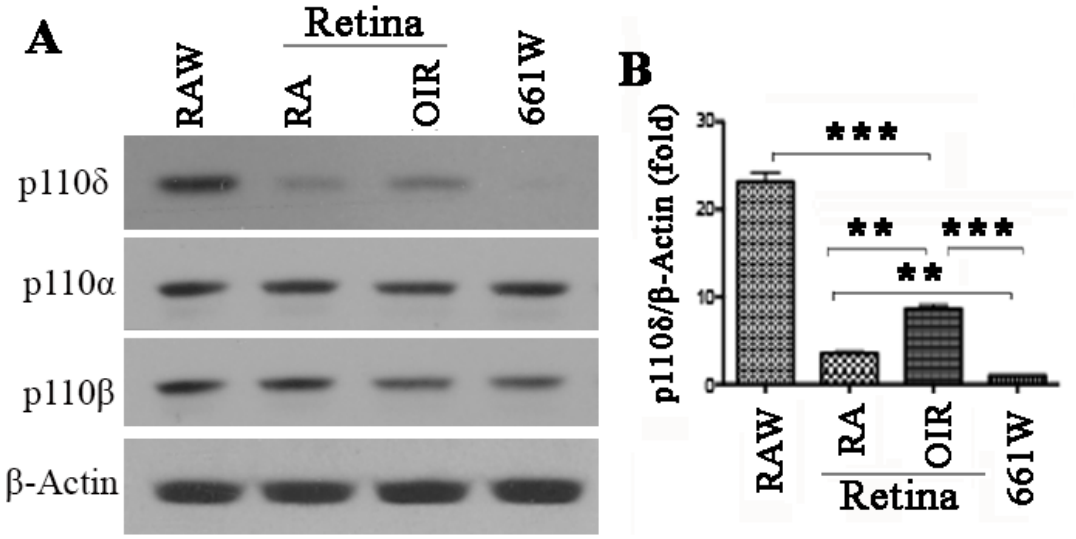

Figure 2

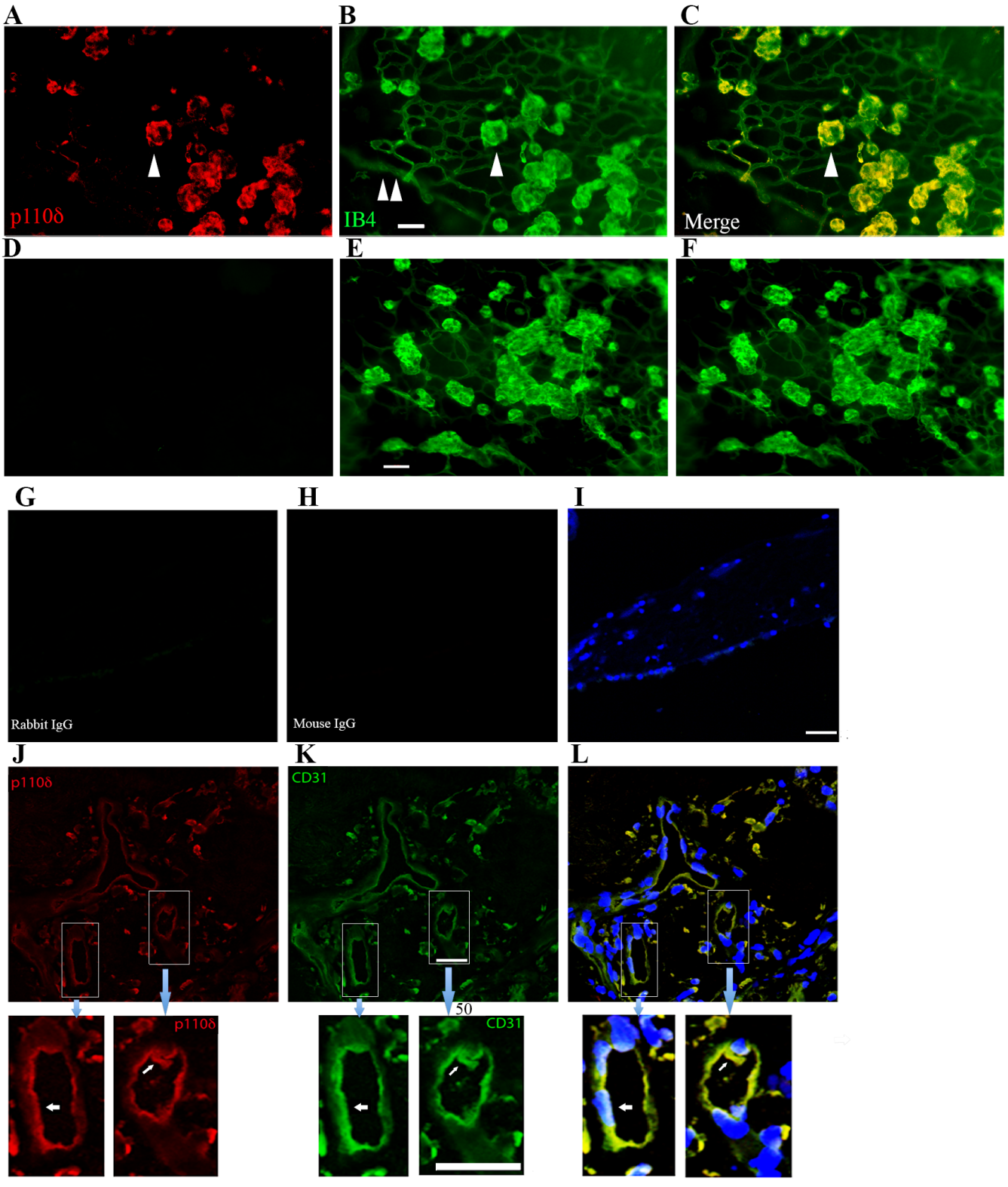
A
B
C
p110δ
IB4
Merge
D
E
F
G
H
I
Rabbit IgG
Mouse IgG
J
K
L
p110δ
CD31
p110δ
CD31
50

Figure 3

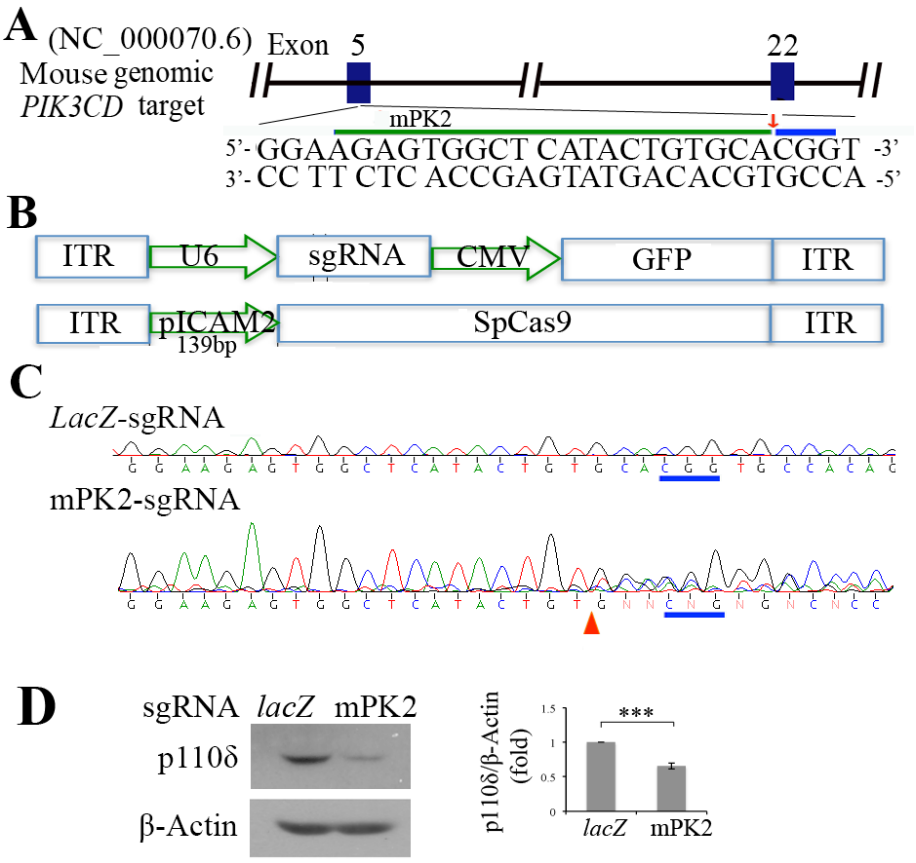
A
(NC_000070.6)
Mouse genomic
PIK3CD target
Exon 5
22
mPK2
5'- GGAAGAGTGGCT CATACTGTGCACGGT -3'
3'- CC TT CTC ACCGAGTATGACACGTGCCA -5'
B
ITR
U6
sgRNA
CMV
GFP
ITR
ITR
pICAM2
139bp
SpCas9
ITR
C
LacZ-sgRNA
mPK2-sgRNA
D
sgRNA lacZ mPK2
p110δ
β-Actin
p110δ/β-Actin (fold)
***
lacZ
mPK2

Figure 4

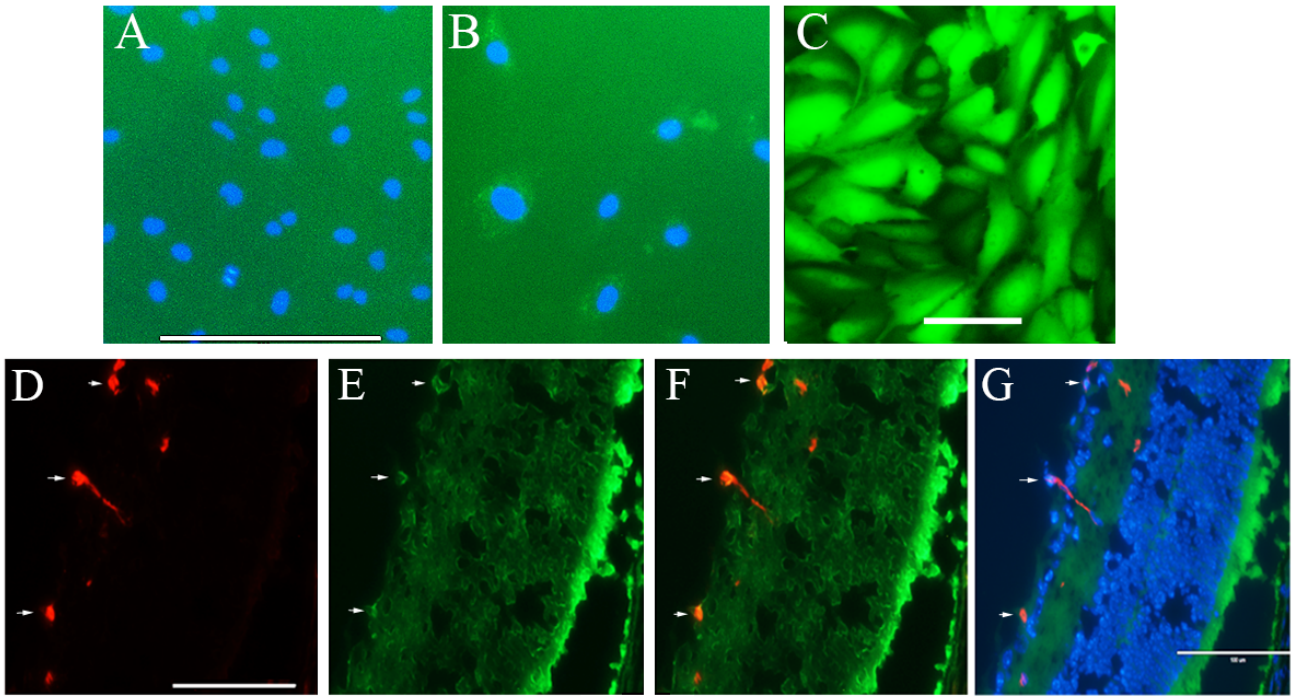

Figure 5

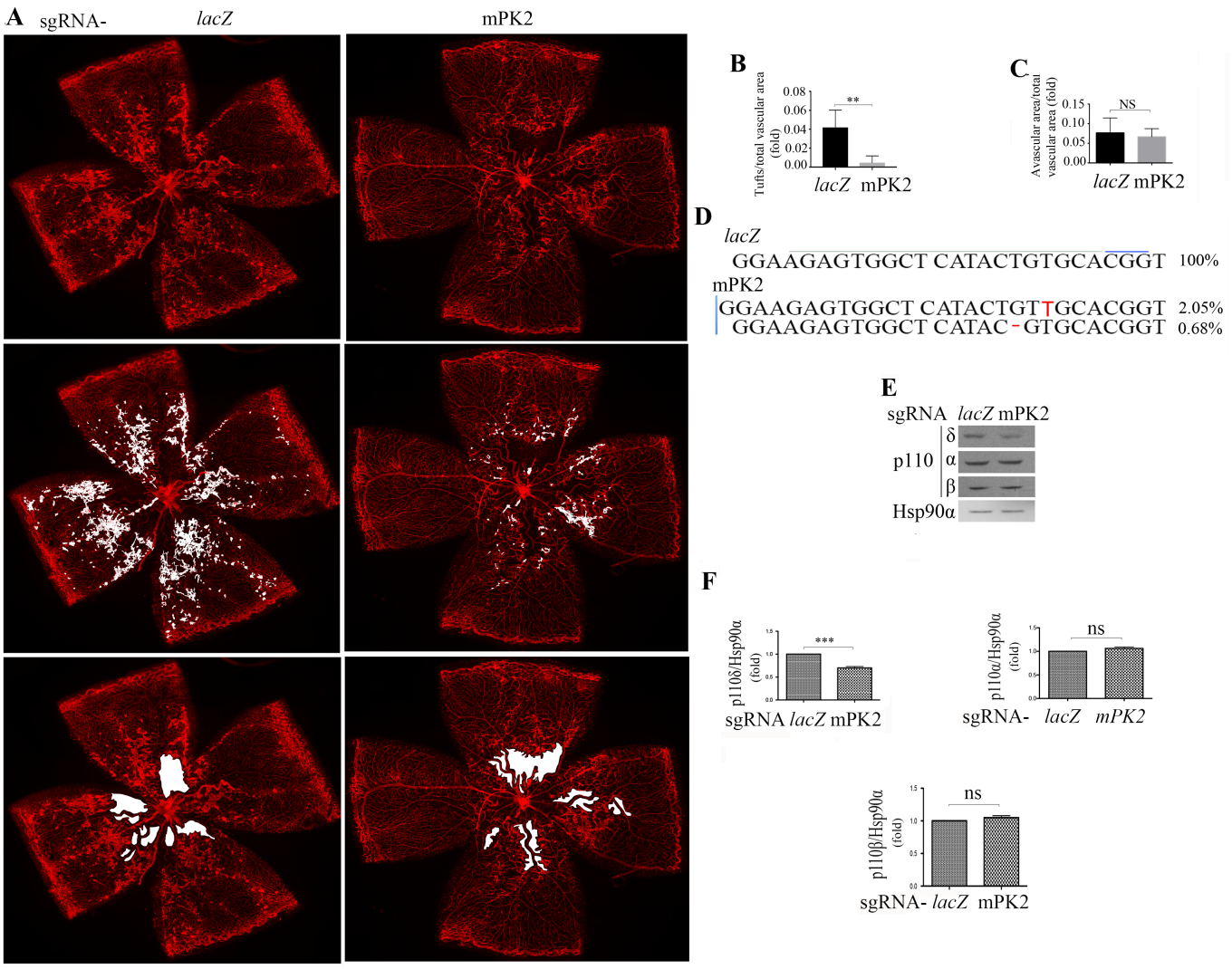
A
sgRNA-
lacZ
mPK2
B
Tufts/total vascular area (fold)
0.08
0.06
0.04
0.02
0.00
**
lacZ
mPK2
C
Avascular area/total vascular area (fold)
0.15
0.10
0.05
0.00
NS
lacZ
mPK2
D
lacZ
GGAAGAGTGGCT CATACTGTGCACGGT 100%
mPK2
GGAAGAGTGGCT CATACTGTTGCACGGT 2.05%
GGAAGAGTGGCT CATAC-GTGCACGGT 0.68%
E
sgRNA lacZ mPK2
p110
δ
α
β
Hsp90α
F
p110δ/Hsp90α (fold)
***
sgRNA lacZ mPK2
p110α/Hsp90α (fold)
ns
sgRNA- lacZ mPK2
p110β/Hsp90α (fold)
ns
sgRNA- lacZ mPK2

Figure 6

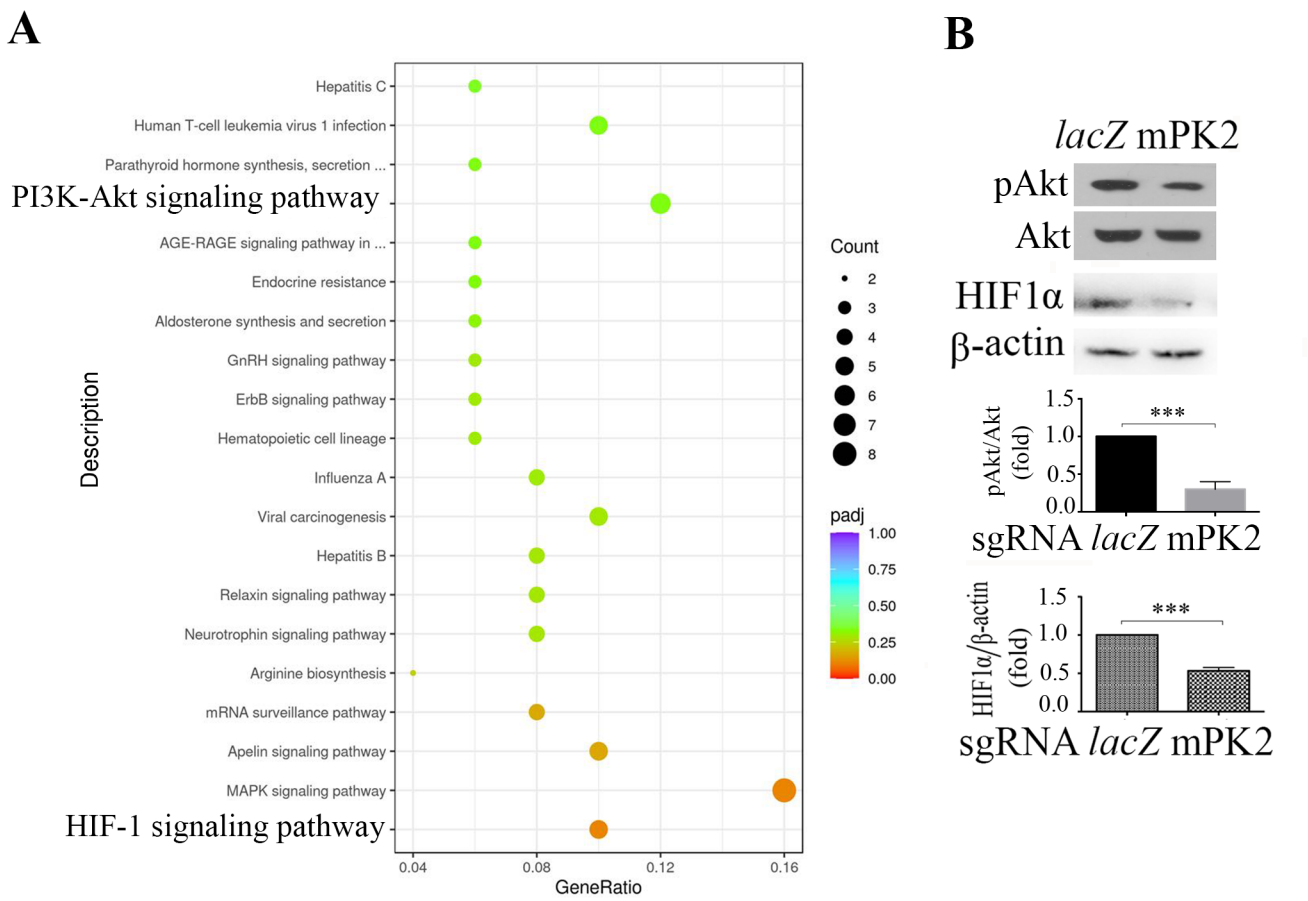
A
Hepatitis C
Human T-cell leukemia virus 1 infection
Parathyroid hormone synthesis, secretion ...
PI3K-Akt signaling pathway
AGE-RAGE signaling pathway in ...
Endocrine resistance
Aldosterone synthesis and secretion
GnRH signaling pathway
ErbB signaling pathway
Hematopoietic cell lineage
Influenza A
Viral carcinogenesis
Hepatitis B
Relaxin signaling pathway
Neurotrophin signaling pathway
Arginine biosynthesis
mRNA surveillance pathway
Apelin signaling pathway
MAPK signaling pathway
HIF-1 signaling pathway
Description
0.04
0.08
0.12
0.16
GeneRatio
Count
2
3
4
5
6
7
8
padj
1.00
0.75
0.50
0.25
0.00
B
lacZ mPK2
pAkt
Akt
HIF1α
β-actin
pAkt/Akt (fold)
1.5
1.0
0.5
0.0
***
sgRNA lacZ mPK2
HIF1α/β-actin (fold)
1.5
1.0
0.5
0.0
***
sgRNA lacZ mPK2

Figure 7

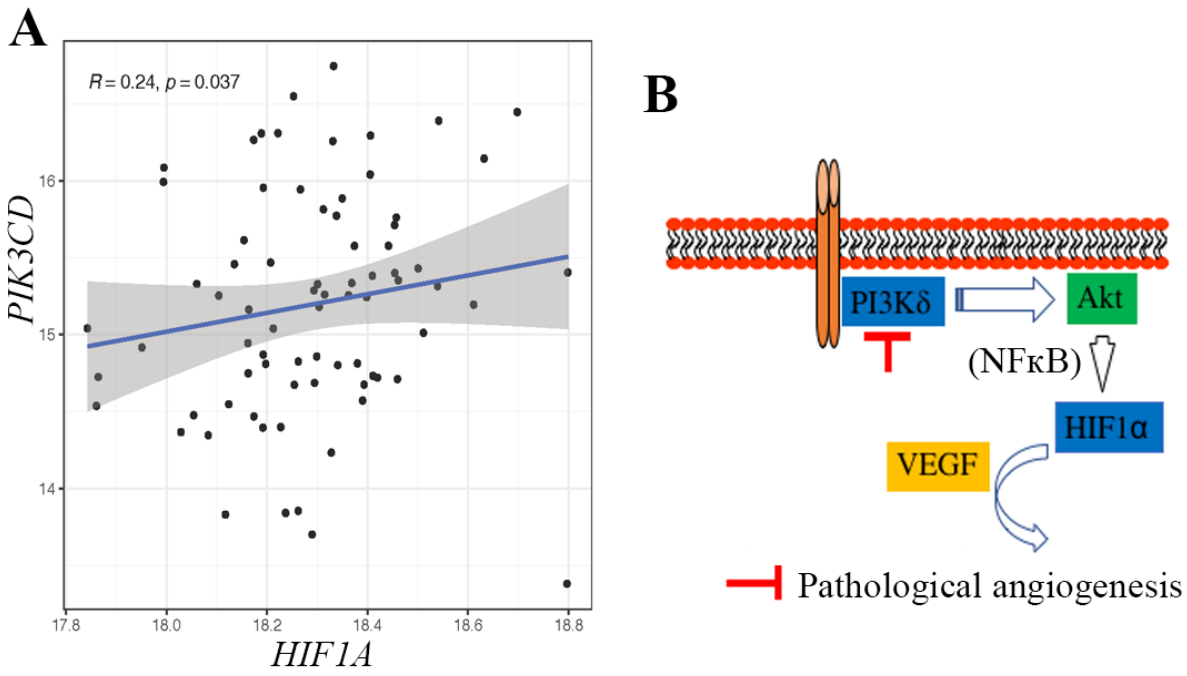
A
R = 0.24, p = 0.037
PIK3CD
HIF1A
16
15
14
17.8
18.0
18.2
18.4
18.6
18.8
B
PI3Kδ
Akt
(NFκB)
HIF1α
VEGF
Pathological angiogenesis